Zhang et al. Journal of Cloud Computing (2023) 12:155
https://doi.org/10.1186/s13677-023-00541-4

Journal of Cloud Computing:
Advances, Systems and Applications

RESEARCH

Open Access

Research on electromagnetic vibration energy harvester for cloud-edge-end collaborative architecture in power grid

Minghao Zhang[1], Rui Song[1†], Jun Zhang[1,2*†], Chenyuan Zhou[3], Guozheng Peng[1], Haoyang Tian[4], Tianyi Wu[4] and Yunjia Li[3]

Abstract

With the deepening of the construction of the new type power system, the grid has become increasingly complex, and its safe and stable operation is facing more challenges. In order to improve the quality and efficiency of power grid management, State Grid Corporation continues to promote the digital transformation of the grid, proposing concepts such as cloud-edge-end collaborative architecture and power Internet of Things, for which comprehensive sensing of the grid is an important foundation. Power equipment is widely distributed and has a wide variety of types, and online monitoring of them involves the deployment and application of a large number of power sensors. However, there are various problems in implementing active power supplies for these sensors, which restrict their service life. In order to collect and utilize the vibration energy widely present in the grid to provide power for sensors, this paper proposes an electromagnetic vibration energy harvester and its design methodology based on a four-straight-beam structure, and carries out a trial production of prototype. The vibration pickup unit of the harvester is composed of polyimide cantilevers, a permanent magnet and a mass-adjusting spacer. The mass-adjusting spacer can control the vibration frequency of the vibration unit to match the target frequency. In this paper, a key novel method is proposed to increase the number of turns in a limited volume by stacking flexible coils, which can boost the output voltage of the energy harvester. A test system is built to conduct a performance test for the prototype harvester. According to the test results, the resonant frequency of the device is 100 Hz, the output peak-to-peak voltage at the resonant frequency is 2.56 V at the acceleration of 1 g, and the maximum output power is around 151.7 μW. The proposed four-straight-beam electromagnetic vibration energy harvester in this paper has obvious advantages in output voltage and power compared with state-of-the-art harvesters. It can provide sufficient power for various sensors, support the construction of cloud-edge-end architecture and the deployment of a massive number of power sensors. In the last part of this article, a self-powered transformer vibration monitor is presented, demonstrating the practicality of the proposed vibration energy harvester.

Keywords Vibration energy harvesting, Electromagnetic, Stacked flexible coils, Polyimide

†Rui Song and Jun Zhang contributed equally to this work.

*Correspondence:
Jun Zhang
zhangjun8@hnu.edu.cn
Full list of author information is available at the end of the article

Introduction

With the deepening of the construction of the new type power system, the power grid is becoming increasingly complex and system stability is facing challenges. Due to their own output characteristics, wind power and photovoltaic power have low reliability, which will lead to insufficient reliable capacity in the power system and a significant decrease in the ability to regulate system frequency. In addition, there is a seasonal mismatch between new energy generation and consumption, resulting in seasonal power balance issues. In order to ensure the stable operation of the power grid and reduce the cost of power transmission, the State Grid Corporation of China has continuously promoted the digital transformation of the grid, proposing concepts such as the power cloud-edge-end collaborative architecture and power artificial intelligence (AI). Data collection with a massive number of sensors is the foundation of power grid digitization, which reflects the operation of the power grid and provides supports for AI models on cloud servers [1–3]. However, due to the wide distribution and diverse types of power equipment, supplying power to sensors poses significant challenges. Especially for power sensors deployed along transmission lines, it is basically impossible to rely on active power sources for power supply, greatly reducing their service life. Therefore, there is an urgent need to solve the problem of powering sensor to meet the needs and support the construction and operation of cloud-edge-end collaborative architecture.

Vibration energy has advantages of wide distribution and low environmental impact and vibration widely exists in power equipment, so it is an important direction to solve the above problem by making use of environmental energy harvesting technology to harvest energy in the environment and convert it into electric energy to supply power to sensors. Vibration characteristics in power scenarios are relatively complex. Vibration of transformers is mainly due to vibration of winding and iron core under the action of electromagnetic force and mechanical force. Vibration characteristics are constant-frequency vibration with multiple frequency points of 100 *Hz* and its frequency doubling [4–7]. The vibration of shunt reactor is mainly caused by Lorentz force on the winding, Maxwell force acting on the surface of the core and magneto strictive effect of the core. Vibration characteristics are also constant-frequency vibrations with multiple frequency points of 100 *Hz* and its frequency doubling [8]. Vibration of capacitors are mainly caused by electrostatic force inside the capacitor, and frequency of vibration is twice that of the external power supply, for example: the frequency of external power supply is 50 *Hz*, and frequency of vibration signal of the capacitor surface is mainly 100 *Hz* [9]. However, vibration intensity of power equipment is relatively weak, so it is key to restrict application of vibration energy harvesting technology to improve its ability to adapt to environmental frequency and its output performance in a limited volume.

Vibration energy harvesting technology can be divided into electrostatic, piezoelectric, electromagnetic, magneto strictive, triboelectric and other forms according to different working principles [10]. Electromagnetic vibration energy harvesting technology has the advantages of no external power supply, large output power and rich material processing technology; an electromagnetic vibration energy harvester is a device that converts relative movement between coil and permanent magnet into electric energy. At present, much research have been made on resonant electromagnetic vibration energy harvesters. When resonant frequency of the device matches the ambient vibration frequency, the device has best output performance. Therefore, it is an important performance objective of electromagnetic vibration energy harvester to adapt to environmental frequency. Vibration frequency of power equipment cannot be changed manually, while resonant frequency of electromagnetic vibration energy harvesters can be adjusted. Mechanical adjustment is a way to adjust frequency of electromagnetic energy harvesters. Resonant frequency of the device can be changed by adjusting key parameters of components, such as geometric parameters of beam [11–13], mass of vibration pickup unit [14–16], stiffness of beam [17–19] and stress of beam [20, 21]. In addition, output voltage and power of the device need to be further improved for practical application of elec-tromagnetic vibration energy harvesters [22–24]. Therefore, improving output voltage and power is another important performance indicator of electromagnetic vibration energy harvesters.

On the basis of existing electromagnetic vibration energy harvesting technology, this paper designs and manufactures an electromagnetic vibration energy harvester based on a four-straight-beam structure, which is mainly composed of a polyimide beam, a permanent magnet, a mass adjustment spacer and a stacked flexible coil. For the vibration environment in power scenarios, the key design objective of the device is to adapt to environmental frequency and improve output performance. In order to adapt to environmental frequency, mass of the vibration pickup unit is adjusted by changing the thickness of the mass adjustment spacer to change resonant frequency of the device and match with target frequency. In order to improve output performance, stacked flexible coils are implemented to increase the number of turns in a limited volume to boost output voltage of the device. To demonstrate the practicality, the proposed energy harvester is integrated with a MEMS (micro-electro-mechanical systems) sensor for monitoring vibrations of power transformers.

System design

System design principle

The electromagnetic vibration energy harvester is a device that converts relative movement between the coil and permanent magnet into electrical energy based on electromagnetic induction phenomenon. The electromagnetic vibration energy harvester is divided into a vibration pickup unit and an energy conversion unit according to different functions of the unit. The vibration pickup unit is mainly composed of a beam and a mass block, which converts vibration in the environment into relative movement between the coil and the permanent magnet. When vibration of the coil is consistent with that of the external environment and the mass of the vibration pickup unit is a permanent magnet, it is called a moving-iron type electromagnetic vibration energy harvester. The energy conversion unit is mainly composed of a coil and a permanent magnet, which converts relative movement of the coil and the permanent magnet into voltage at both ends of the coil, and can generate output power during the connection with a load.

Movement characteristics of vibration pickup unit of electromagnetic vibration energy harvesters can be analyzed by a spring-mass-damping model. According to Newton's second law, the second-order movement equation of a vibration pickup unit is as follows:

$$m\frac{\mathrm{d}^2\mathrm{z(t)}}{\mathrm{dt}^2}+(c_\mathrm{e}+c_\mathrm{m})\frac{\mathrm{dz(t)}}{\mathrm{dt}}+k\mathrm{z(t)}=\mathrm{m}\omega^2\mathrm{Ysin}(\omega\mathrm{t}) \tag{1}$$

Where, m refers to mass of the mass (permanent magnet), c_e refers to the electro-magnetic damping coefficient of the system, c_m refers to the mechanical damping coefficient of the system, k refers to the elastic coefficient of the spring, $z(t)$ refers to dis-placement of the mass (permanent magnet), $Y(t)$ refers to environmental vibration displacement, and ω refers to angular frequency of environmental vibration displacement. System damping of electromagnetic vibration energy harvesters are composed of electromagnetic damping (c_e) and mechanical damping (c_m). Electromagnetic damping (c_e) comes from ampere force exerted on the coil by induced current generated when the coil moves in a magnetic field, and mechanical damping (c_m) mainly comes from thermoelastic damping of the spring material. When the two damping components are equal, the device can output maximum power under conditions of resonant frequency and matching impedance.

Assuming the coil and the permanent magnet in the electromagnetic vibration energy harvester complete one-dimensional relative movement in z direction, according to Faraday's law of electromagnetic induction, the induced voltage $E(t)$ in the coil is as follows:

$$E(t)=-N\frac{\mathrm{d}\phi}{\mathrm{dt}}=-NA\frac{\mathrm{dB}}{\mathrm{d}z}\frac{\mathrm{dz}}{\mathrm{d}t} \tag{2}$$

Where, N refers to the number of turns, ϕ refers to magnetic flux, B refers to magnetic induction intensity, and A refers to area of the coil. Formula (2) ignores the gradient of magnetic induction intensity in x and y directions, because when the distance between the coil and the permanent magnet is very close, the ratio of magnetic induction intensity in x and y directions to z direction is relatively small, so this approximation is feasible. According to Formula (2), induced voltage in the coil can be expressed as the product of the number of turns (n), effective area of the coil (a), mag-netic induction intensity gradient $\left(\frac{\mathrm{dB}}{\mathrm{dz}}\right)$ and vibration speed $\left(\frac{\mathrm{dz}}{\mathrm{d}t}\right)$.

Output voltage of the device in a finite volume needs to be further improved for the practical application of electromagnetic vibration energy harvesters. According to Formula (2), optimizing the number of turns (n) and increasing vibration speed $\left(\frac{\mathrm{dz}}{\mathrm{d}t}\right)$ of vibration pickup unit are helpful to boost output voltage of the device. However, at present, the processing process of the multi-layer coil in electromagnetic vibration energy harvesters mainly, includes an electroplating process, thick film process and printed circuit board process. Electroplating process and thick film process have the disadvantages of high processing cost and difficulty, while the printed circuit board process features low cost, but fails to change number of turns flexibly. In addition, vibration speed of vibration pickup parts is usually limited by stiffness of the beam.

On the basis of existing electromagnetic vibration energy harvesting technology, this paper designs and manufactures an electromagnetic vibration energy harvester based on a four-straight-beam structure. The stacked flexible coil and a polyimide beam are adopted to boost output voltage of the device from the above two aspects. Based on flexible printed circuit board processing technology, the stacked flexible coil increases the number of turns in a limited volume, and has the advantages of low processing cost and flexible change of coil layers. The vibration pickup part, made of polyimide with low Young's modulus, increases vibration speed of the vibration pickup part. In addition, adapting to environmental frequency is another important performance indicator of resonant electromagnetic vibration energy harvesters. When the resonant frequency of the device matches the ambient vibration frequency, the device has the best output performance. This paper adjusts mass of the vibration pickup unit by changing thickness of mass adjustment spacer to change the resonant frequency of the device and match the target frequency.

Analytical model

Number of straight beam supports on the beam affects resonant frequency and vibration mode of the vibration pickup unit. Increase of the number of straight beams can be equivalent to parallel connection of multiple springs. After parallel connection, stiffness of the beam increases, increasing resonant frequency of the vibration pickup unit. Increase of the number of straight beams also enhances symmetry and stability of the vibration pickup unit. Due to asymmetry of the supporting beams, first-order vibration modes of vibration pickup units supported by a single straight beam and double straight beams are twisted, instead of an up-and-down vibration mode along the z axis direction. First-order vibration modes of vibration pickup units supported by three straight beams and four straight beams are up-and-down vibration modes along the z axis direction, and resonant frequency of the vibration pickup unit with four-straight-beam structure is larger. When mass of the vibration pickup unit increases, resonant frequency of the vibration pickup unit decreases. In order to facilitate frequency adjustment of the vibration pickup unit, this paper adopts the beam with four-straight-beam structure.

The straight beam of vibration pickup with rectangular cross section in electro-magnetic vibration energy harvester can be analyzed by a fixed-guided model, as shown in Fig. 1. For the beam, the left side is a fixed end, with a displacement of 0; the right side is a guided end with a tip mass, with vertical movement only. Considering the number of supports of the plane beam is 4, the tip mass is equivalent to 1/4 of the mass of the vibration pickup unit (m).

Under small disturbances, the movement equation of homogeneous beam can be described by Formula (3) [25]:

$$\frac{\partial^4 V(x,t)}{\partial x^4} + \frac{\rho}{EI}\frac{\partial^2 V(x,t)}{\partial t^2} = 0 \tag{3}$$

Where, $V(x, t)$ refers to displacement of the straight beam at position (x) at time (t), and ρ, E and I refer to mass per unit length of the straight beam, Young's modulus and area moment, respectively.

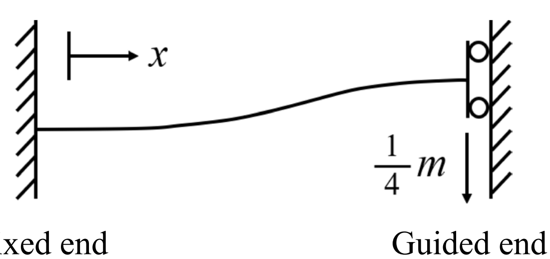

Fig. 1 Schematic diagram of the fixed-guided model

Assuming the straight beam performs vibration at the angular frequency (ω), the displacement expression of the straight beam is as follows:

$$V(x,t) = v(x)\sin(\omega t) \tag{4}$$

After Formula (4) is substituted into Formula (3) to obtain the movement equation independent of time (t), and boundary conditions of the device are substituted into the formula, the following characteristic equation can be obtained by sorting.

$$-\frac{m\omega^2}{2EI} + \frac{m\omega^2}{2EI}\cosh(\beta l)\cos(\beta l) + 2\beta^3\sinh(\beta l)\cos(\beta l) + 2\beta^3\cosh(\beta l)\sin(\beta l) = 0 \tag{5}$$

Where, coefficient (β) is a quantity about the angular frequency of vibration, geometric parameters and material parameters of the beam, it is $\beta = (\rho\omega^2/EI)^{1/4}$. The solution of the characteristic Eq. (5) can be obtained by using polyimide as the material of the beam and substituting geometric parameters and material parameters of the vibration pickup unit in Table 1. The relation curve between mass of the vibration pickup unit (m) and resonant frequency of the device ($f = \omega/2\pi$) obtained by calculating the analytical model is shown in Fig. 2. As shown in the figure, with increase of the mass of the vibration pickup unit (m), resonant frequency of the device gradually decreases. When mass of the vibration pickup unit (m) is 6 g, resonant frequency of the device is 122.5 Hz; when mass of the vibration pickup unit (m) increases to 9 g, resonant frequency of the device decreases to 100.1 Hz.

Finite element model

COMSOL finite element simulation software is used to a make modal analysis on the vibration pickup unit with thickness of the mass adjustment spacer of 1 mm (corresponding to the mass of the vibration pickup unit (m) of 7.7 g); results are shown in Fig. 3. In the model, the constraint structure of FR4 plates, bolts and screws in the actual device is simplified by imposing fixed constraints on the frame outside the four straight beams on the plane beam. Modes of the first four orders are up-and-down

Table 1 The parameters of the vibration pickup element model

Parameter	Value
Beam length (l) (mm)	4.5
Beam width (b) (mm)	1
Beam thickness (h) (mm)	0.3
Young's modulus (E) (GPa)	3.0
Mass per unit length (ρ) (kg/m)	4.32×10^{-4}
Mass of vibration pickup unit (m) (g)	$6 \sim 9$

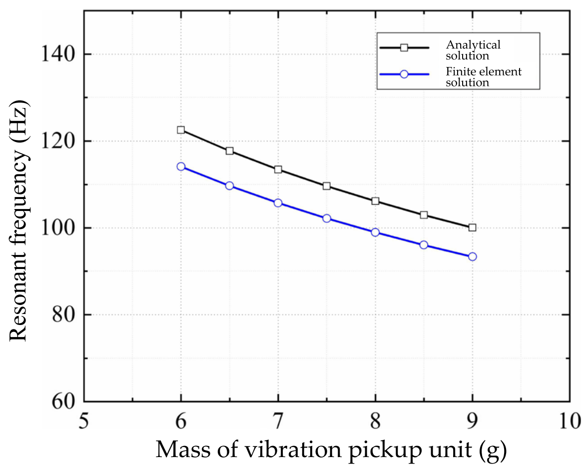

Fig. 2 Resonant frequency as a function of quality of the vibration pickup element

vibration mode (103.6 *Hz*), torsion mode around *y* axis (104.6 *Hz*), torsion mode around *x* axis (104.8 *Hz*) and in-plane torsion mode around *z* axis (417.7 *Hz*). Because vibration direction of the external excitation is in the *z* axis and components of the vibration pickup unit are symmetrically designed, upper and lower vibration modes are the main vibration modes of the device.

The relation curve between the mass of the vibration pickup unit (*m*) and resonant frequency of the device obtained by calculating the finite element model is shown in Fig. 2. As shown in the figure, curves of analytical solution and finite element solution have the same change trend. With increase of mass of vibration pickup unit (*m*), resonant frequency of the device obtained by analytical model and finite element model decreases gradually. However, the analytical solution is about 7 *Hz* larger than the finite element solution. The reason may be different distribution of mass of vibration pickup unit in the two models, and mass of vibration pickup unit in the analytical model is equivalent to a mass point at the guided end; however, in the finite element model, mass of the vibration pickup unit is distributed on the butterfly surface of the beam.

Because of deviation in actual geometric parameters, material parameters and design parameters of electromagnetic vibration energy harvesters, the analytical model and finite element model cannot accurately predict resonant frequency of the device, but the two models provide approximate resonant frequency of the designed electromagnetic vibration energy harvester and influencing effect of the mass of the vibration pickup unit (*m*) on resonant frequency.

Model prototype and experimental platform

Model prototype

Electromagnetic vibration energy harvesters designed based on a four-straight-beam structure is shown in Fig. 4. The four-straight-beam vibration energy harvester is a

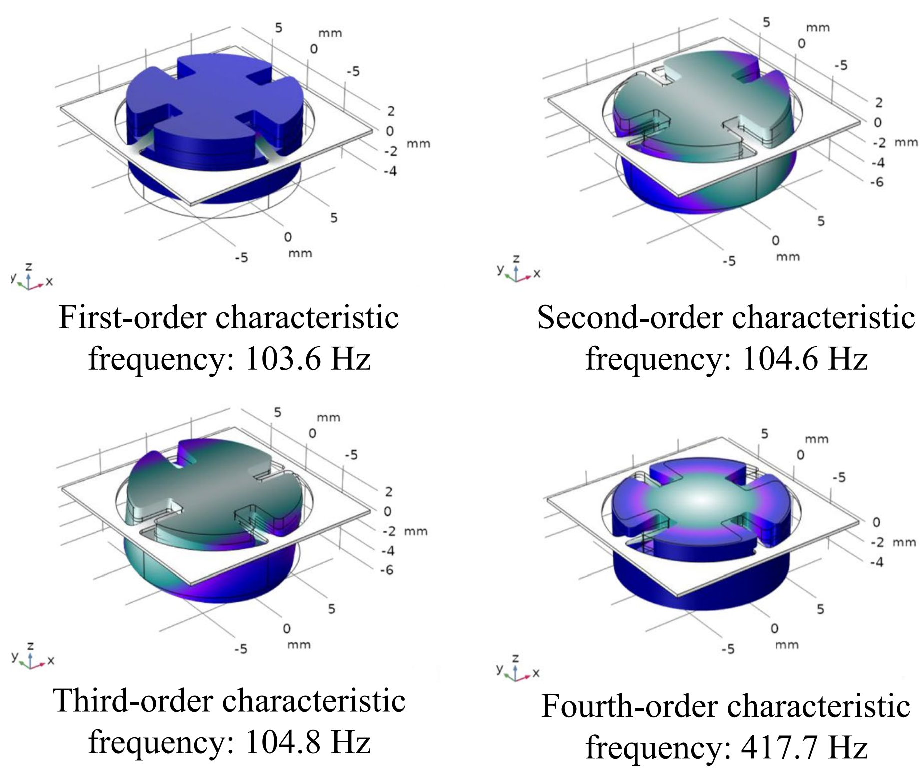

Fig. 3 Modal analysis of the vibration pickup element

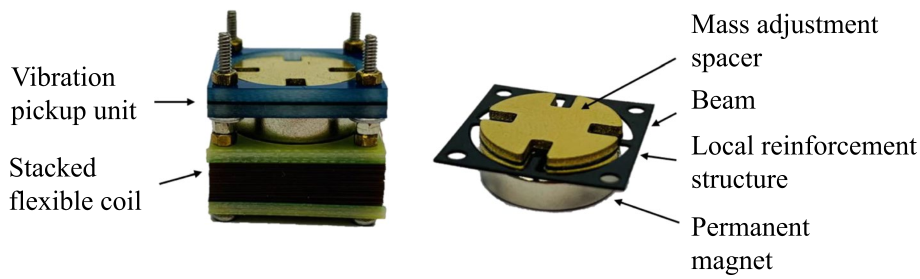

Fig. 4 Photograph of energy harvester

moving-iron type vibration energy harvester, which is mainly composed of two parts: One is a vibration pickup unit composed of a beam, permanent magnet, local reinforcement structure and mass adjustment spacer, the other is an energy conversion unit composed of stacked flexible coils. The vibration pickup unit and the energy conversion unit are fixed by the combination of FR4 circuit boards, bolts and screws. Through-hole pads on FR4 circuit boards are connected with electrodes of stacked flexible coils, to realize electrical connection, which is convenient for signal output and measurement. The mass adjustment spacer, beam, local reinforcement structure and permanent magnet of the vibration pickup unit are stuck together in sequence. The butterfly reinforcement structure not only prevents material from hardening due to glue overflow in the sticking process, but also effectively prolongs length of the beam. In addition, quality change of the vibration pickup unit is realized by brass mass adjustment spacers with different heights, thereby changing resonant frequency of the vibration pickup unit. Key parameters of the device are shown in Table 2. N52 NdFeB magnet is used as the permanent magnet, and residual magnetism is $1430 \sim 1460\ mT$. Other key parameters of the permanent magnet are shown in Table 3.

Table 2 Key Parameters of the vibration energy harvester

Parameter	Value
Size of beam (*mm*^{3})	$19 \times 19 \times 0.3$
Length of straight beam (*mm*)	4.5
Width of straight beam (*mm*)	1.0
Thickness of mass adjustment spacer (*mm*)	1.0
Thickness of local reinforcement structure (*mm*)	1.0
Diameter of permanent magnet (*mm*)	14.9
Height of permanent magnet (*mm*)	3.9
Number of turns of single-layer coil (*turn*)	98
Line width of spiral copper coil (*mm*)	0.075
Line thickness of spiral copper coil (*mm*)	0.018
Number of coil layers (*pieces*)	39
Coil resistance (ω)	1350
Distance between coil and permanent magnet (*mm*)	1.3
Shell size (*mm*^{3})	$31 \times 31 \times 40$

Structural design of the single-layer flexible coil in the prototype of the vibration energy harvester designed is shown in Fig. 5. Based on flexible printed circuit board processing technology, the flexible coil has the advantages of low cost, small volume and flexible change of turns. The middle of the flexible coil is a double-layer spiral copper coil, and upper and lower sides are copper electrodes and dummy electrodes respectively, ensuring symmetry of the coil structure and further ensuring convenience of assembly. The double-layer spiral copper coil realizes electric connection through the middle through hole. There is also a rectangular polyimide reinforcement structure on one side of the dummy electrode, to ensure reliable electrical connection during assembly of the multi-layer flexible coil. Number of turns can be doubled when a plurality of flexible coils are stacked together and connected in series. Number of turns of the combined coil is realized by changing the number of flexible coils. Resistance of 39 flexible coils is 1350 Ω upon experimental test.

The vibration energy harvester with shell packaged is shown in Fig. 6. The shell of the vibration energy harvester is composed of an upper cover plate, a pipe wall and a lower cover plate, with length, width and height of 31 mm, 31 mm and 40 mm, respectively, and made from aluminum materials treated by black anodic oxidation, to ensure good protection in outdoor environments. Bolts and nuts are used to first install the vibration energy harvester on the boss in the pipe wall, and then install the circuit part on the lower cover plate, finally fixing the upper cover plate and lower cover plate on the pipe wall, to complete integrated assembly of the prototype. The vibration energy harvester is mainly composed of

Table 3 Performance parameters of the N52 NdFeB magnet

Performance indicator	Parameter
Brand	*N52*
Residual magnetism (*mT*)	$1430 \sim 1460$
Magnetic coercivity (*kA/m*)	≥ 836
Intrinsic coercivity (*kA/m*)	≥ 955
Maximum magnetic energy product (kJ/m^3)	$390 \sim 422$
Maximum operating temperature (°*C*)	80

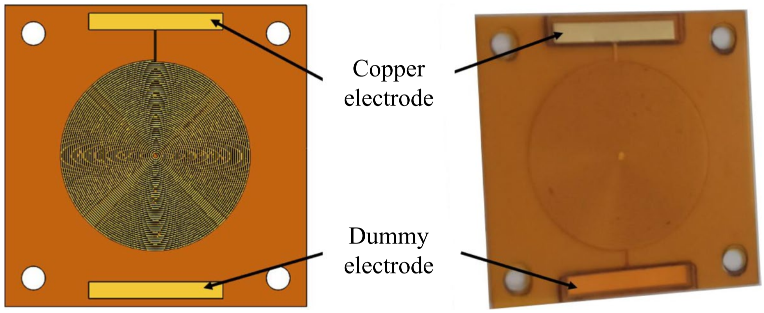

Fig. 5 Layout diagram and photograph of single-layer flexible coil

Fig. 6 Photograph of vibration energy harvester with package shell

two parts: One is a vibration pickup unit composed of a beam, a permanent magnet, a local reinforcement structure and mass adjustment spacer, the other is an energy conversion unit composed of stacked flexible coils.

Test system

As shown in Fig. 7, the test system of the electromagnetic vibration energy harvester design is composed of a modal vibration exciter, a signal generator, a power amplifier, an accelerometer, a data acquisition card and a computer. In performance characterization experiment, external excitation vibration is generated by the modal vibration exciter, and its vibration characteristics are determined by signal generator and power amplifier, and the accelerometer measures vibration data. The output of accelerometer and electromagnetic vibration energy harvester is acquired by a data acquisition card and transmitted to computer, and then processed by LabVIEW software. In the system test, sinusoidal voltage signal is used as excitation. Model and performance parameters of the experimental equipment selected for the test system are shown in Table 4.

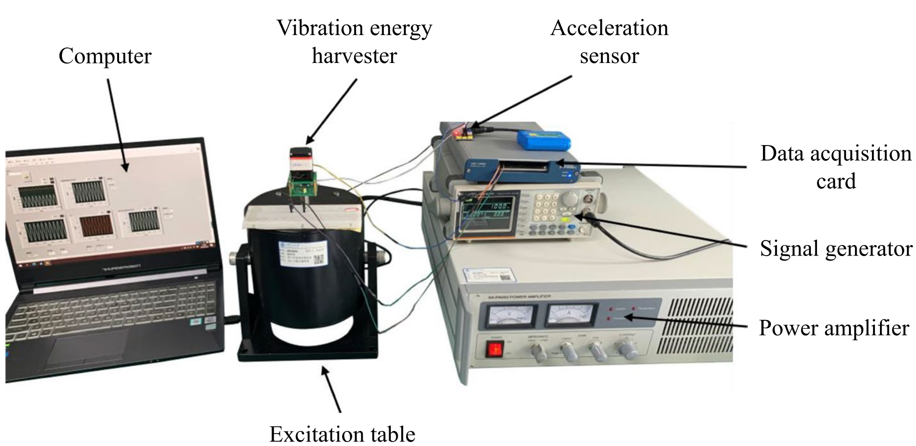

Fig. 7 Photograph of the test system

Table 4 The parameters of the experimental equipment

Equipment model	Performance parameter
JZK-20 modal vibration exciter	Maximum amplitude: ±10*mm*
	Maximum excitation force: 200*N*
AFG-2112 signal generator	Resolution: 0.1*Hz*
	Frequency range of sine wave and square wave: 0.1 ∼ 12*MHz*
SA-PA050 YE 5873A power amplifier	Frequency response: 0 ∼ 50*kHz* ± 1*dB*
ADXL335 accelerometer	Measuring range: ±3*g*
	Sensitivity: 330*mV/g*
NI USB-6343 data acquisition card	Maximum sampling rate: 500*kS/s*

Results and discussion

Influence of mass of vibration pickup parts on resonant frequency of device

Figure 8 is the variation trend of the measured values of the resonant frequency of the device under different masses of the vibration pickup unit and variation curve of resonant frequency calculated by the analytical model and finite element model. Resonant frequency of the device under 4 different vibration pickup units has been tested. Mass of vibration pickup unit is adjusted by changing thickness of mass adjustment spacer. When mass of the vibration pickup unit is 5.7 g, 6.4 g, 7.0 g and 8.3 g, resonant frequency of the device is 108 Hz, 100 Hz, 98 Hz and 92 Hz, respectively. According to the curve in the figure, resonant frequency of the device obtained by experimental test and model calculation decreases with increase of mass of the vibration pickup unit, and variation trend of the resonant frequency test curve, analytical model and finite element model calculation curve is consistent.

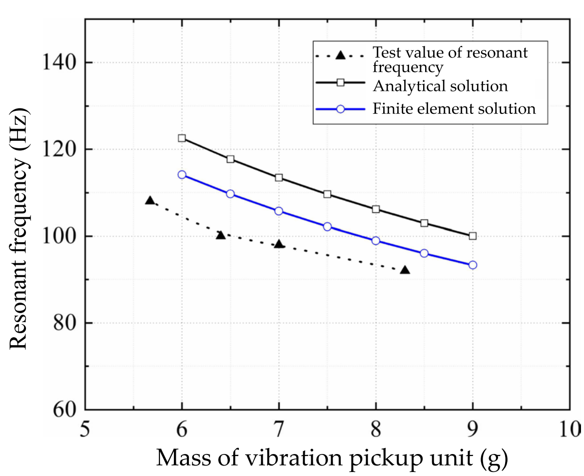

Fig. 8 Resonant frequency as a function of quality of the vibration pickup element

Measured resonant frequency of the device is lower than calculated by analytical model and finite element model, and reasons may be as follows: 1. There are deviations in actual geometric parameters, material parameters and design parameters of the device, for example, machining accuracy of vibration pickup piece cut by laser is 0.1 *mm*; 2. During vibration of the mass of the vibration pickup unit, the beam is under axial stress, which will make the stiffness of the beam nonlinear and make the beam harden or soften, and nonlinear influence is not considered in the analytical model and finite element model; 3. The mass adjustment spacer, beam, local reinforcement structure and permanent magnet of vibration pickup unit are glued together in turn with acrylic glue, and the influence of acrylic glue is not considered in analytical model and finite element model.

Influence of excitation frequency on output voltage of device

Figure 9 shows the curve of relationship between output peak-to-peak voltage and the excitation frequency of the electromagnetic vibration energy harvester when excitation acceleration is 1 g. As shown in the figure, resonant frequency of the device is 100 Hz, and corresponding output peak-to-peak voltage is 2.56 V. When excitation frequency is close to resonant frequency of the device, the peak-to-peak output voltage increases; when excitation frequency is far away from resonant frequency of the device, the output peak-to-peak voltage decreases rapidly. When resistance of the external resistor is equal to that of the internal resistance of the energy harvester, maximum output power can be obtained, and the formula is as follows:

$$P_{\max} = \frac{V_{\mathrm{RMS}}^2}{R_{\mathrm{L}}} = \frac{V_{\mathrm{PP}}^2}{8R_{\mathrm{L}}} \tag{6}$$

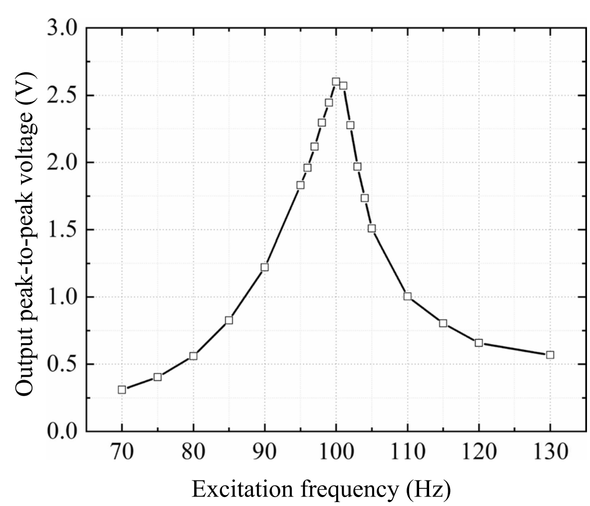

Fig. 9 Sweep frequency curve of output voltage of electromagnetic vibration energy harvester

Where, V_{RMS} refers to effective value of output voltage, V_{PP} refers to output peak-to-peak voltage, and R_L refers to resistance value of load. Internal resistance of the combined coil of the device is 1350 Ω. Under resistance matching, upon theoretical calculation, maximum output power of the device is 151.7 μW under acceleration of 1 g.

Figure 10 is a curve of output voltage of the device changing with time at the resonant frequency of 100 Hz and nearby frequencies. As shown in the figure, when excitation frequency is 100 Hz, output peak-to-peak voltage of the device is maximum; when excitation frequency is far away from 100 Hz, output peak-to-peak voltage gradually decreases. When excitation frequency is 100 Hz, peak values of the positive half wave and negative half wave of the corresponding time domain waveform in the figure are 1.30 V and 1.26 V, respectively. The reason for the slight distortion of the time domain waveform band is mass of the vibration pickup unit is large, and displacement of the vibration pickup unit during downward vibration is slightly larger than during upward vibration, so the peak value of waveform on one side is larger than of the waveform on the other side. This waveform asymmetry is more obvious when excitation acceleration is large. In addition, when the excitation signal is sinusoidal signal, output voltage presents an approximate sinusoidal curve regardless of whether excitation frequency is the resonant frequency of the device.

Influence of excitation acceleration on output voltage of device

Figure 11 shows the curve of the relationship between output peak-to-peak voltage and the root-mean-square value and excitation acceleration of the electromagnetic vibration energy harvester when excitation frequency is 100 Hz. As shown in the figure, when excitation acceleration is in the range of 0.2 g to 1 g, output voltage of the energy harvester is directly proportional to excitation acceleration; when excitation acceleration is in the range of 1 g to 2 g, output voltage of the energy harvester decreases with growth rate of excitation acceleration. This is because distance between the combined coil and magnet in the experiment is 1.3 mm, which is applicable to vibration energy harvesting with acceleration of 1 g or below. The Schematic Diagram for Upward/ Downward Vibration of the vibration pickup unit is shown in Fig. 12. When acceleration is greater than 1 g, the polyimide beam collides with the upper surface edge of the magnet during upward vibration, causing output voltage of the energy harvester decreases with growth rate of the excitation acceleration.

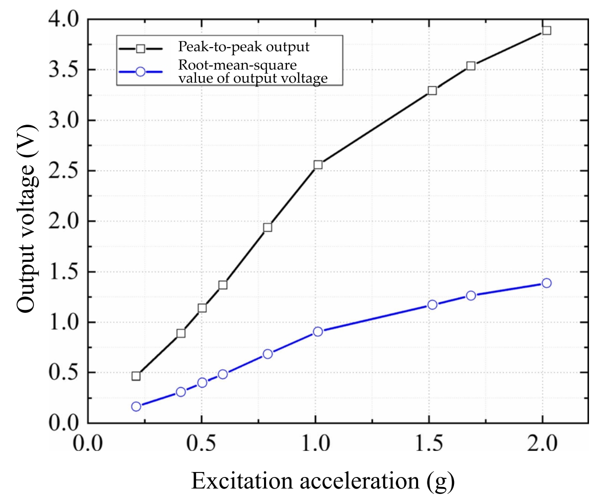

Fig. 11 Sweep acceleration curve of output voltage of electromagnetic vibration energy harvester

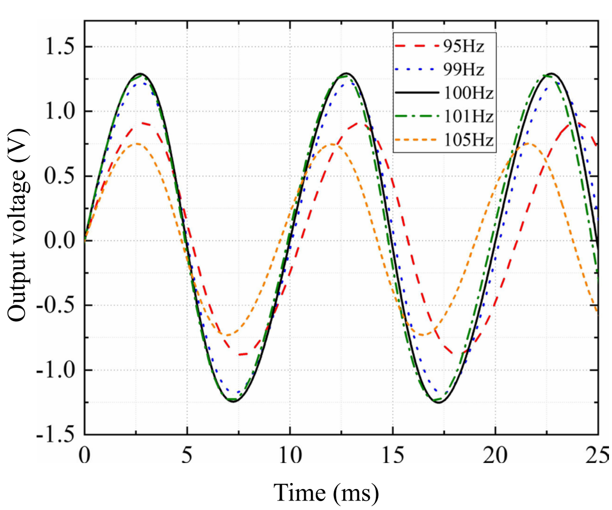

Fig. 10 Time domain waveform of output voltage of electromagnetic vibration energy harvester under different excitation accelerations

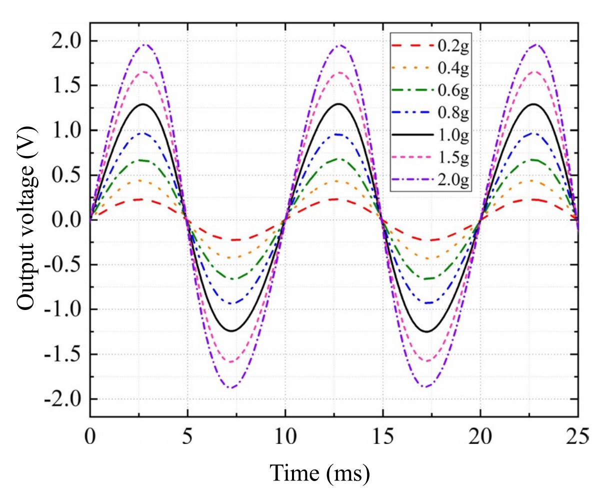

Fig. 12 Schematic diagram of the vibration pickup element

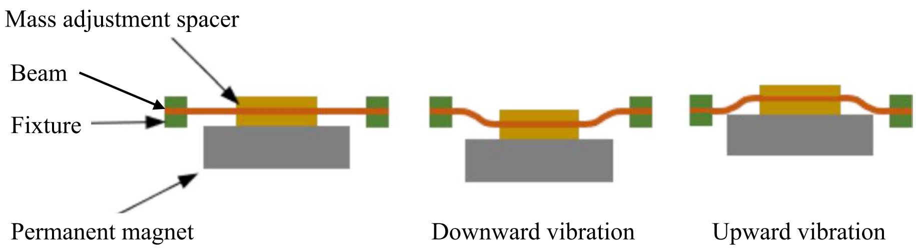

Fig. 13 Time domain waveform of output voltage of electromagnetic vibration energy harvester under different excitation accelerations

Figure 13 is a curve of the output voltage of the device changing with time at excitation acceleration of 0.2 g to 2 g. As shown in the figure, when excitation acceleration increases from 0.2 g to 2 g, output peak-to-peak voltage of the device gradually increases, and waveform of the output voltage is approximately sinusoidal. When excitation acceleration is 0.2 g, peak values of the positive half wave and negative half wave of time domain waveform are 0.23 V and 0.23 V, respectively; when excitation acceleration is 1 g, peak values of the positive half wave and negative half wave of the time domain waveform are 1.30 V and 1.26 V, respectively; when excitation acceleration is 2 g, peak values of the positive half wave and negative half wave of the time domain waveform are 1.98 V and 1.89 V, respectively. With increase of excitation acceleration, peak value difference between positive and negative half waves increases, and waveform asymmetry is more obvious. The reason for asymmetry of positive and negative time domain waveforms is the vibration pickup unit is affected by gravity during vibration, and displacement during downward vibration is slightly larger than during upward vibration. When excitation acceleration is large, upward vibration amplitude of the beam is limited by distance between the beam and the upper surface of the magnet.

Performance comparison of electromagnetic vibration energy harvester

Output performance of vibration energy harvester is generally expressed by normalized performance coefficient FOM ($\mu W/g^2/gram^2$) and normalized power density NPD ($\mu W/g^2/cm^3$). Expressions are as follows:

$$FOM = \frac{P}{A^2 m^2} \quad (7)$$

$$NPD = \frac{P}{A^2 V} \quad (8)$$

Where, P refers to output power of vibration energy harvester, A refers to amplitude of excitation acceleration, m refers to mass of the vibration pickup unit, and V refers to volume of vibration energy harvester. Table 5 compares performance of vibration energy harvesters. According to analysis, four vibration energy harvesters, with resonant frequencies of less than 200 Hz, are all applicable to power scenarios with low frequency. Compared with other related research results, the electromagnetic vibration energy harvester based on the four-straight-beam structure proposed in this paper has obvious advantages in output voltage, power, FOM and NPD.

A self-powered vibration monitor for power transformers based on the proposed energy harvester

To demonstrate the functionality and practicality of the proposed harvester, a self-powered vibration monitor was manufactured and tested. It mainly consists of a vibration energy harvester, a power management unit, a vibration monitoring unit and a rechargeable lithium battery pack, as illustrated in Fig. 14. The power management unit uses the ADP5091 chip, which can utilize ultra-low energy with a voltage as low as 80 mV and provide it to the back-end system

Table 5 Comparison of output performance between the devices

References	[22]	[23]	[24]	This article
Excitation acceleration (g)	-	2	3	1
Resonant frequency (Hz)	10.2	66	108	100
Output peak-to-peak voltage (V)	1.52	1.57	0.89	2.56
Output power (μW)	-	91.8	68	151.7
FOM ($\mu W/g^2/gram^2$)	-	3.53	11.83	10.23
NPD ($\mu W/g^2/cm^3$)	-	23.48	13.43	84.04

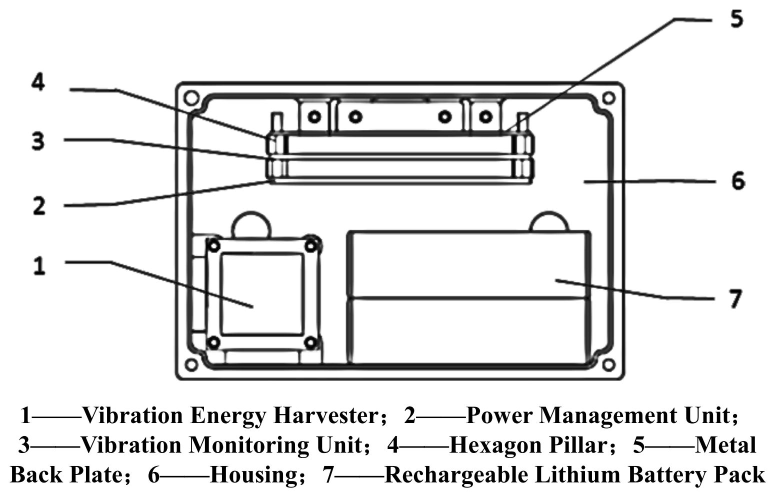

Fig. 14 Internal structure diagram of the self-powered vibration monitor for transformers

application with a conversion efficiency of up to 90% or more. At the same time, its static current can be controlled at around 500 *nA*.

Vibration monitoring unit integrates ADXL1002 (Analog Devices, inc.) MEMS accelerometer for vibration sensing, Cortex-M4 (ARM Holdings, plc.) for signal processing and an RF (radio frequency) transceiver complying IEEE 802.15.4 for communication. Powered with 3.3V supply, the total power consumption can be estimated as $\sim 117\ \mu W$.

Photographs of the vibration monitor is shown in Fig. 15. It can be directly attached to the power transformers through the permanent magnets set at the back of the housing. After calibration and validation, a vibration monitor was deployed at a 220 kV transformer substation on Poyang Road, Tianjin, China. The proposed energy harvester worked well and could generate sufficient power to fed the monitor. Figures 16 and 17 shows the data taken from one of the 220 kV transformers in operation, and in Fig. 17 the 100 Hz component can be clearly observed.

Conclusion

For power equipment scenarios, this paper proposes a design method of electromagnetic vibration energy harvester based on a four-straight-beam structure. For difficulty of matching the target frequency, this paper adjusts resonant frequency of the device by changing mass of the vibration pickup unit. For the problem of low output voltage of energy harvester, this paper adopts stacked flexible coils, to increase the effective number of turns and boost output voltage of the device. According to the experiment, resonant frequency of the four-straight-beam electromagnetic vibration energy harvester is 100 Hz, output peak-to-peak voltage at the resonant frequency is 2.56 V at

Fig. 15 Photographs of the self-powered vibration monitor for transformers

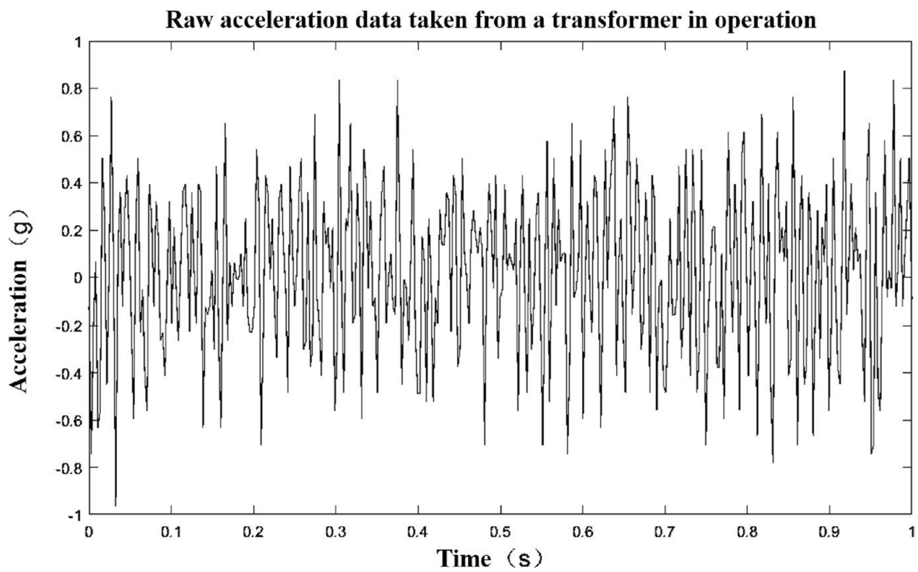

Fig. 16 Raw acceleration data taken by the deployed vibration monitor

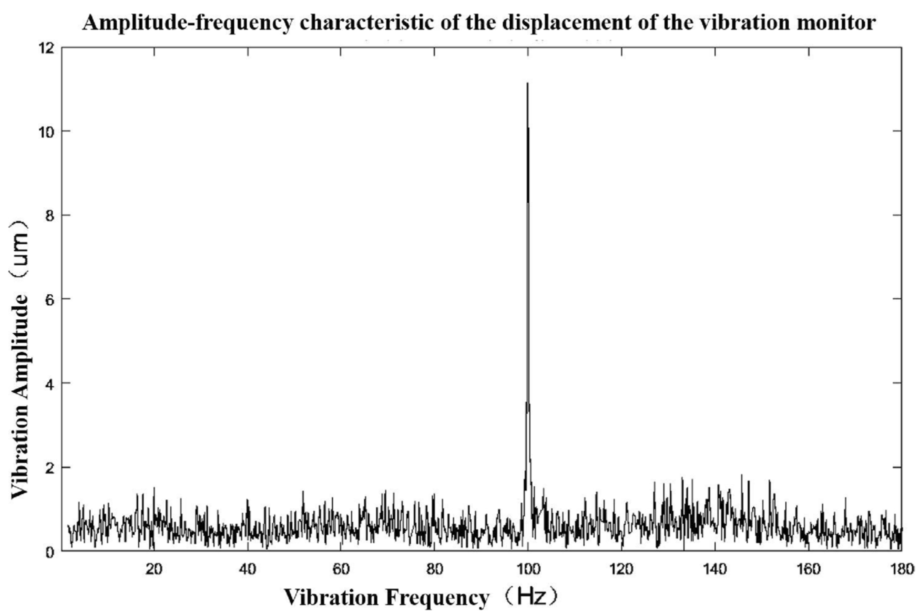

Fig. 17 Amplitude-frequency characteristic of the displacement of the deployed vibration monitor

the acceleration of 1 g, and maximum output power is 151.7 μW under matching resistance upon theoretical calculation. The four-straight-beam electromagnetic vibration energy harvester in this paper has obvious advantages in output voltage and power compared with domestic and foreign output performance of electromagnetic vibration energy harvesters in recent years. The application of the proposed energy harvester in a vibration monitor has proven its practicality.

Acknowledgements

The work presented in this paper was funded by the State Grid Corporation of China through the Science and Technology Project under Grant (52094020006Z). The author of this paper is very grateful to LI Yunjia from Xi'an Jiaotong University for valuable advice on the calculation model; the author's sincere thanks also go to Dr. ZHOU Chenyuan from Xi'an Jiaotong University for great help for device tests and performance analysis!

Authors' contributions

Minghao Zhang: Conceptualization, Methodology, Validation, Formal analysis, Writing - Original Draft. Rui Song: Hardware, Fabrication, Validation, Formal analysis, Resources, Writing - Review & Editing. Jun Zhang: Formal analysis, Resources, Modelling, Hardware, Fabrication, Validation, Deployment. Chenyuan Zhou: Modelling, Fabrication, Validation, Testbench design. Guozheng Peng: Validation, Formal analysis, Deployment. Haoyang Tian: Writing - Review & Editing, Supervision, Project administration, Funding acquisition. Tianyi Wu: Writing - Review & Editing, Supervision, Project administration, Funding acquisition. Yunjia Li: Conceptualization, Writing - Review & Editing, Supervision, Project administration, Funding acquisition.

Authors' information

Minghao Zhang graduated from Xi'an Jiaotong University in 2016 with a M.S. degree in Mechanical Manufacturing and Automation. He is primarily engaged in the research of online monitoring and disaster prevention technologies related to power transmission line.

Rui Song received the B.Eng. degree in electrical engineering and automation from North China Electric Power University, Beijing, China, in 2014, and the M.Sc. degree in electronics and the Ph.D. degree in integrated micro and nano systems from the University of Edinburgh, Edinburgh, U.K., in 2015 and 2019, respectively. He is currently an Engineer with China Electric Power Research Institute Company Ltd. His research interests include analog and mixed-signal electronics, power edge intelligence and smart sensing.

Jun Zhang received the B.S. degree in electrical engineering and automation from North China University of Science and Technology, Tangshan, China, in 2013, and the M.S. degree with Northeast Electric Power University, Jilin, China, in 2016. He is currently pursuing the Ph.D. degree in electrical engineering, Hunan University, Changsha, China. He is also with China Electric Power Research Institute Company Ltd. His current research interests include power edge intelligence and smart sensing.

Chenyuan Zhou is currently working on online monitoring of power transmission lines.

Guozheng Peng received B.S. and the M.S. degrees in electrical engineering and automation from the North China Electric Power University, Beijing, in 2003 and 2006. He is a Senior Engineer with China Electric Power Research Institute Company Ltd. His research interests include power edge intelligence and smart sensing.

Yunjia Li is currently working on online monitoring of power transmission lines.

Funding

This work was supported by the State Grid Corporation of China through the Science and Technology Project under Grant (52094020006Z).

Declarations

Competing interests

The authors declare no competing interests.

Author details

[1]China Electric Power Research Institute, Haidian District, Beijing 100192, China. [2]College of Electrical and Information Engineering, Hunan University, Yuelu District, Changsha 410082, China. [3]School of Electrical Engineering, Xi'an Jiaotong University, Xianning West Road, Xi'an 710049, China. [4]State Grid Shanghai Municipal Electric Power Company Electric Power Research Institute, Hongkou District, Shanghai 200437, China.

Received: 27 September 2023 Accepted: 3 November 2023
Published online: 13 November 2023

References

1. Lv L (2021) Design and implementation of online monitoring system for power equipment operation status. Equip Manag Maint 488(2):128–129
2. Lu L, Zhu W (2021) Application of power internet of things technology in online monitoring of power equipment. Inf Technol 356(7):155–159
3. Wang B, Xie J (2019) Application of power internet of things sensor technology in online monitoring of power equipment. J State Grid Technol Coll 22(4):37–40
4. Shi Y, Ji S, Zhang F (2019) Research on the operation deformation mode shape characteristics of transformer oil tank surface. Chin J Electrotech Technol 34(5):1088–1095
5. Li B, Wang Z, Liu H (2021) Experimental study on vibration and noise of 500kv single-phase transformer under dc bias. J Electrotech Technol 36(13):2801–2811
6. Pan C, Su H, Cai G (2020) Research on the vibration characteristics of abnormal current in transformers under dc bias. Chin J Electrotech Technol 35(9):1868–1879
7. Zhu L, Wang B, Liu S (2018) Analysis of the influence of different loads on the electromagnetic vibration of dry-type transformers. J Electrotech Technol 33(7):1599–1606
8. Zhang P, Li L, Cheng Z (2018) Vibration simulation and test comparison of shunt reactor and transformer model iron core. J Electrotech Technol 33(22):5273–5281
9. Cao T, Ji S, Wu P (2010) Calculation method of capacitor noise level based on vibration signal. J Electrotech Technol 25(6):172–177
10. Mu J (2021) Design and experimental research of composite vibration energy harvester for self-powered monitoring system [d]. North Central University, D Taiyuan
11. Mösch M, Fischerauer G, Hoffmann D, (2020) A self-adaptive and self-sufficient energy harvesting system. Sensors-Basel 20(9):2519
12. Tyagi N, Gaur A, Mahajan A (2022) Performance evaluation of novel piezoelectric cantilever beam structure for energy harvesting. Trends Sci 19(22):836
13. Bouhedma S, Hu S, Schütz A, Lange F, Mohammed O, Bechtold T, Hohlfeld D, (2022) Analysis and characterization of optimized dual-frequency vibration energy harvesters for low-power industrial applications. Micromachines 13(7):1078
14. Pradeesh EL, Udhayakumar S, Vasundhara MG (2021) Design and development of frequency tuneable vibration based piezoelectric energy harvester. Ferroelectrics 584(1):85–99
15. Li Y, Zhou C, Wang X, Wang J, Qiao D, Tao K (2022) A vibration energy harvester with targeted frequency-tuning capability. IEEE Trans Instrum Meas 71(1):1–10
16. Li Y, Wang X, Zhang S, Zhou C, Qiao D, Tao K (2021) A pendulum-like low frequency electromagnetic vibration energy harvester based on polymer spring and coils. Polymers 13(19):3380
17. Deng L, Jiang J, Zhang D (2021) Design and modeling a frequency self-tuning vibration energy harvester for rotational applications. Energy 235:121414
18. Wang S, Li Z, Zhang H, Fang S, Zhou S (2023) Analytical and experimental investigation of a flexible bistable energy harvester in rotational environment. Nonlinear Dyn 111:16851–16873
19. Zhang Y, Wang W, Xie J, Lei Y, Cao J, Xu Y, Bader S, Bowen C, Oelmann B (2022) Enhanced variable reluctance energy harvesting for self-powered monitoring. Appl Energy 321(119):402
20. Li Y, Zhou C, Cao Q (2021) Electromagnetic vibration energy harvester with tunable resonance frequency based on stress modulation of flexible springs. Micromachines 12:1130
21. Wang X, Li J, Zhou C, Tao K, Qiao D, Li Y (2021) Vibration energy harvester based on torsionally oscillating magnet. Micromachines 12(12):1545
22. Jiang Y, Song F, Xiong Y (2022) Collision-type piezoelectric vibration energy harvester in low frequency environment. Light Ind Mach 40(2):97–102
23. Li Y, Cao Q, Zhang W (2018) A miniaturized electromagnetic energy harvester with volt-level output based on stacked flexible coils. Smart Mater Struct 27(11):115040
24. Khan F, Sassani F, Stoeber B (2014) Nonlinear behaviour of membrane type electromagnetic energy harvester under harmonic and random vibrations. Microsyst Technol 20(7):1323–1335
25. Shaker J (1975) Effect of axial load on mode shapes and frequencies of beams. NASA Technical Note. No. E-8433.

Publisher's Note